Influence of Ce^{3+} substituted Calcium silicate for WLEDs and Display applications

Kamala Soppin[1], P. Krishna Murthy[2], B. M. Manohara[3,*]

[1]*Department of Physics, DRM Science College, Davangere - 577004, India.*
[2]*Department of Physics, Government Science College, Chitradurga - 577501, India.*
[3]*Department of Physics, Government First Grade College, Davangere - 577004, India.*

Abstract

The Ce^{3+} substituted $CaSiO_3$ nanophosphors (1-7 mol %) have been synthesized by using solution combustion technique. Phosphors have been well reported by Powder X-Ray Diffraction, Field Emission Scanning Electron Microscope, Fourier Transform Infrared Spectroscopy and Ultra Violet Visible Spectroscopy. Powder X-Ray Diffraction patterns reveal monoclinic $CaSiO_3$ phase which can be obtained for calcining the samples at 900 ◦C for 3 h and average size of the samples is (34-42) nm as calculated by Scherer's formula and Williamson-Hall plots. Field Emission Scanning Electron Microscope micrographs show that crystallites are of agglomerated and irregular in shape. Fourier Transform Infrared spectroscopic analysis is to determine the chemical functional groups in the sample. The band gap was evaluated by Kubelka-Munk method is in the range of (3.3-3.4) eV shows semiconducting nature. Photoluminescence of the phosphors were recorded for excitation wavelength at 350 nm show characteristic emission 483 nm of transition 5d →4f of the Ce^{3+} ions. Commission International De I'Eclairage and Coordinated Color Temperature values are situated in the blue regions, prepared phosphor might be useful in Blue component of White Light Emitting Diodes and solid state display applications.

Keywords: DRS; FTIR; Emission spectra; Quenching; WLED; Display applications;

1. INTRODUCTION

The advance of environmental protection and energy conservation awareness, developing green and environment-friendly lighting source becomes increasingly important. White-light emitting diodes (W-LEDs), more preferable candidates for replacing conventional incandescent and fluorescent lamps, have gained considerable attention owing to their attractive advantages of excellent stability, high luminous efficiency, long service life as well as environmental friendliness. Ce^{3+} substituted $CaSiO_3$ nanophosphors prepared by Solution Combustion technique is low temperature (500 ^{0}C) with calcined (heating/sintered) at 900 ^{0}C for 3 hr. compared to solid-state process and Sol-gel method [1-5]. Recently growing academic interest has been focused on the research of pursuing single-component white-light emitting phosphors to gain better color rendering index and small color aberration [6-9].

The properties of the Ce^{3+} ions were directly affected by the static and dynamic properties of their environment and the associated optical spectra was characterized by both sharp and broad emission bands since 5d electrons was outside of the ion core [10]. The improvement of luminescence materials dealt with $CaSiO_3$: Ce^{3+} as an outstanding host due to Ce^{3+} ions cans easily alternative in $CaSiO_3$ and an appropriate host lattices crystal area strength around Ce^{3+} ions. For blue

photoluminescence, trivalent cerium ion (Ce^{3+}) turned into an emitting center because of its emission from 700 to 1400 nm, which contain the R-line narrowband emission around 700 nm and the broadband 483 nm emission from the 5d - 4f transition relying on the host crystal field strength [11-13].

The present work $CaSiO_3:Ce^{3+}$ (1-7 mol %) phosphor has been synthesized by self propagating combustion synthesis (CS) method. The CS technique turned into rapid and able to generating manoclinic section compounds at nano level. There are no reports available on the synthesis and photoluminescence study of $CaSiO_3:Ce^{3+}$ (1-7 mol %) via CS process with Citric acid as a fuel. The character and structural information of the synthesized phosphor become examined by way of powder X-ray diffraction (PXRD), Field emission scanning electron microscopy (FESEM), Fourier transform infrared spectroscopy (FT-IR) techniques. The properties of $CaSiO_3:Ce^{3+}$ nanophosphor was investigated by diffused reflectance spectra (DRS) of UV – Visible Spectrophotometer and photoluminescent (PL) studies.

2 EXPERIMENTAL

2.1 Preparation of $CaSiO_3:Ce^{3+}$ nanophosphor

(1-7 mol %) Ce^{3+} substituted Calcium silicate nanophosphors were prepared by combustion technique by Citric acid as a fuel [14]. The flow chart for the preparation of $CaSiO_3:Ce^{3+}$ (1-7 mol %) was revealed in Fig.1. Analar grade Calcium nitrate ($Ca(NO_3)_2{\cdot}4H_2O$; Sigma Aldrich, 99.9 %), fumed silica (SiO_2, 99.9 %), Cerium nitrate ($Ce(NO_3)_3$, 99.9 %) and Citric acid ($C_6H_8O_7$) have been used because the starting materials. The stoichiometric quantity of $Ca(NO_3)_2{\cdot}4H_2O$, SiO_2 and $C_6H_8O_7$ (1:1:1.25 in mole ratio) have been well dissolved in ~100 ml of deionized water and stirred nicely the usage of magnetic stirrer to get homogenized aqueous solution. The combination was heated in a muffle furnace temperature at 500 ± 10 ^oC. The last product became similarly calcined at 900 ^oC for 3 h for the formation of properly crystalline sample. The chemical reaction equation is,

$$(1-x)Ca(NO_3)_2 + x\,RE(NO_3)_3 + C_6H_8O_7 + SiO_2 \rightarrow Ca_{1-x}RE_x\,SiO_{3(s)} + 2CO_{2(g)} + 3H_2O_{(g)} + \left(\frac{3-x}{2}\right)N_{2(g)} \quad \text{---------- (1)}$$

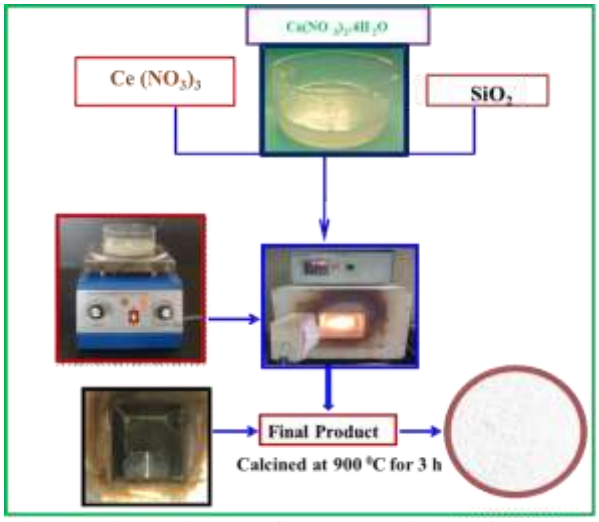

Fig.1. Flow chart of preparation of (1-7 mol%) Ce^{3+} substituted $CaSiO_3$ nanophosphor calcined at 900 ^oC for 3 h.

Table.1. Estimated structural parameter values in undoped and (1-7 mol%) Ce^{3+} substituted $CaSiO_3$ nanophosphor.

Sl. No.	mol %	Scherer's equation. in nm.	W-H Plot. in nm.	Lattice strain $\varepsilon \times 10^{-3}$
01	Pure	38	40	0.24
02	1	35	42	0.46
03	3	34	39	0.43
04	5	36	39	0.29
05	7	40	42	0.22

2.2 Characterization

Powder X-ray diffraction (PXRD) analysis was performed using X'PERT pro Philips analytical diffractometer (operating at 50 KV & 20 mA by means of CuK_α (1.541Å) radiation with an nickel filter at a scan rate of 2^o min^{-1}). The data were collected within the range of 20^0 to 60^0. Morphology of the samples was examined by means of the use of a field emission scanning electron microscope (FESEM) (ULTRA55, FESEM (Carl Zeiss) with EDS). Fourier transform infrared (FTIR) spectra had been recorded in absorption mode with Perkin Elmer spectrometer (Spectrum 1000) together with KBr pellets. The UV visible optical absorption examine of the sample was made in the range (200 - 800 nm) using Perkin Elmer Lambda 19 to attain diffused reflectance spectra (DRS). Photoluminescence (PL) research are made the use of Agilent technologies, model Cary Eclipse, Spectrofluorimeter at room temperature (RT).

3. Results and Discussion

3.1 Powder X-Ray Diffraction (PXRD)

In Fig. 2 PXRD patterns of (1-7 mol %) of Ce^{3+} substituted Calcium silicate calcined at 900 ^oC for 3 h. Diffraction peaks of Ce^{3+} substituted Calcium silicate were properly-matched with the JCPDS card No. 84-0655 [15] and shows well crystalline and single phase. The average crystallite size was predicted by using the Scherrer's formula [16, 17]. Average crystallite size of Ce^{3+} substituted Calcium silicate calcined at 900 ^oC for 3 h was in the range 34 - 40 nm.

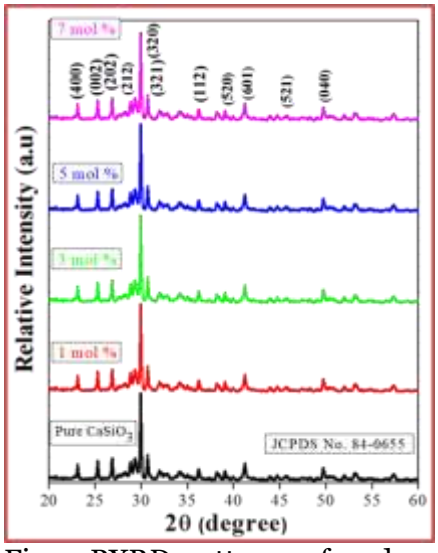

Fig.2. PXRD patterns of undoped and (1-7 mol%) Ce^{3+} substituted $CaSiO_3$ nanophosphor calcined at 900 ^oC for 3 h.

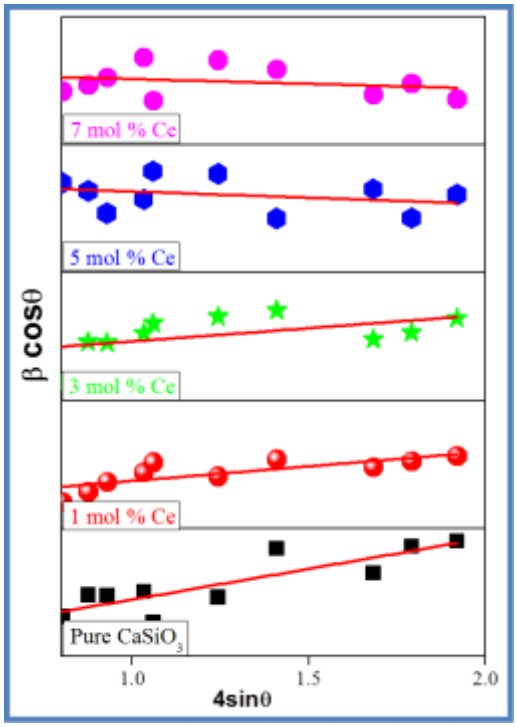

Fig.3. W-H plots of undoped and (1-7 mol%) Ce^{3+} substituted $CaSiO_3$ nanophosphor the lattice strain is extracted from the slope and the crystalline size is extracted from the y-intercept of the fit.

Lattice strain present in the (1-7 mol %) $CaSiO_3:Ce^{3+}$ nanophosphor calcined at 900 ºC for 3 h nanophosphor synthesised was predicted by using Williamson–Hall (W–H) plots [18, 19]. The particle size and lattice strain were taken into consideration may be predicted from the extrapolation of the plot as shown in Fig.3. The average crystallite size and lattice strain predicted from these techniques of the linear fit had been proven in Table 1 and show nano in size.

3.2 Morphological analysis

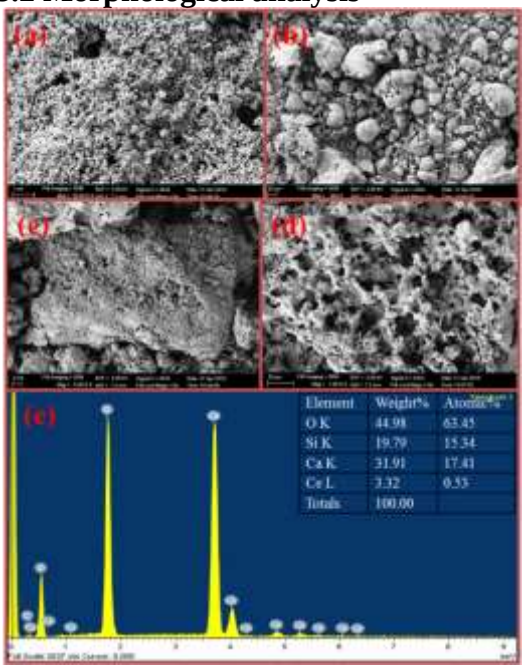

Fig.4. FESEM micrographs of (a) 1 mol% (b) 3 mol% (c) 5 mol% (d) 7 mol% and (f) EDAX (3 mol%) and inset table shows elemenst with atomic weight % of Ce^{3+} substituted $CaSiO_3$ nanophosphor.

Field effect electron scanning microscopes (FESEM) had been an essential tool for the characterization of nanomaterials, as they provide data about the synthesized samples. FESEM and energy dispersive X-ray analysis (EDAX) of $CaSiO_3$**:** Ce^{3+} (1-7 mol %) nanophosphor calcined at 900 ºC for 3 h were showed in Fig.4 (a-e). It was determined that the sample was enormously porous, agglomerated, voids and fluffy with polycrystalline in nature. The pores and voids may be attributed to the massive number of gases escaping out of the reaction mixture throughout combustion.

3.3 Fourier transformation infrared (FTIR) spectroscopy

FTIR analysis is to determine the chemical functional groups in the sample prepared and recorded in the range 4000-400 cm^{-1} shown in Fig.5. The region between 1000 and 1500 cm^{-1} is characterized by an overlapping Si–O. Different bands can be distinguished at 1009, 1081 and 1483 cm^{-1}, which are assigned to various Si–O bonds. The sharp band from 888 cm^{-1} is due to asymmetric stretching vibration of Si-O-Si band and stretching vibrations of terminal Si-O bands. The absorption at 448, 555 and 643 cm^{-1} is due to symmetric stretching vibrations Si-O-Si bridges [20]. The absorption peak at 2351 cm^{-1} shows the existence of hydroxyl groups.

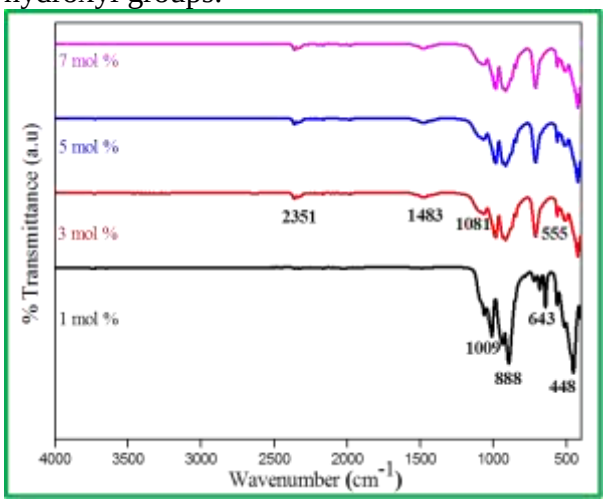

Fig.5. FTIR of (1-7 mol %) Ce^{3+} substituted $CaSiO_3$ nanophosphor.

3.4 UV-Visible absorption

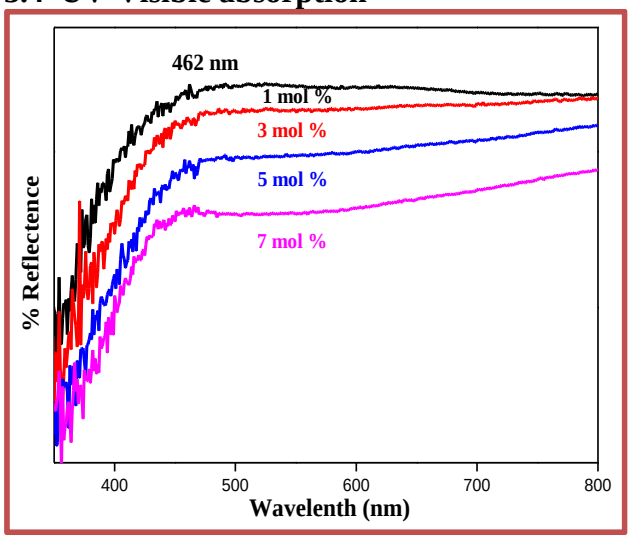

Fig.6. UV Visible DRS spectra of (1-7 mol %) Ce^{3+} substituted $CaSiO_3$ nanophosphor

The UV–Vis absorption spectra of $CaSiO_3$**:** Ce^{3+} (1-7 mol %) nanophosphor calcined at 900 ^{0}C for 3 h samples were shown in inset Fig. 6. Those outcomes in the formation of voids can purpose absorption bands within the UV region, the surface of nanoparticles were widely known to include of numerous defects and absorption of impurity bring about the absorption of nanocrystals. Band gap (E_g) was evaluated by Kubelka- Munk method, DRS of the material changed into converted to the absorption spectra by the usage of Kubelka – Munk function [22] and the band gap value as showed in Fig.7. Predicted value of E_g were in the range of (3.3 – 3.4) eV. Due to this synthesized sample were indicates semiconductor nature.

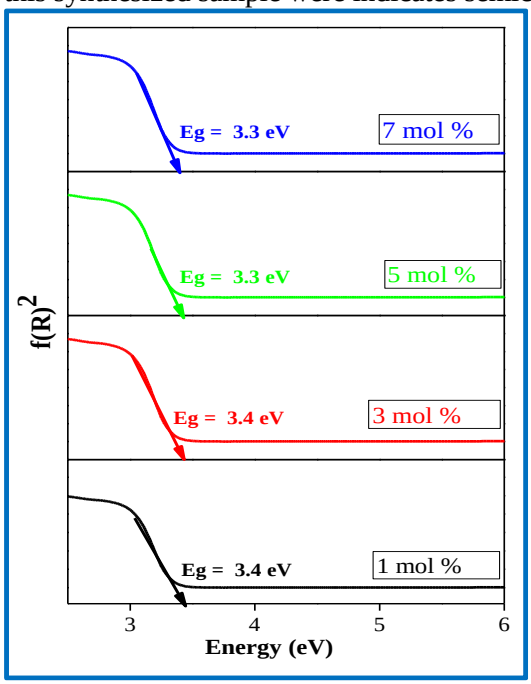

Fig.7. Energy band gap of (1-7 mol %) Ce^{3+} substituted $CaSiO_3$ nanophosphor

3.5 Photoluminescence (PL) studies

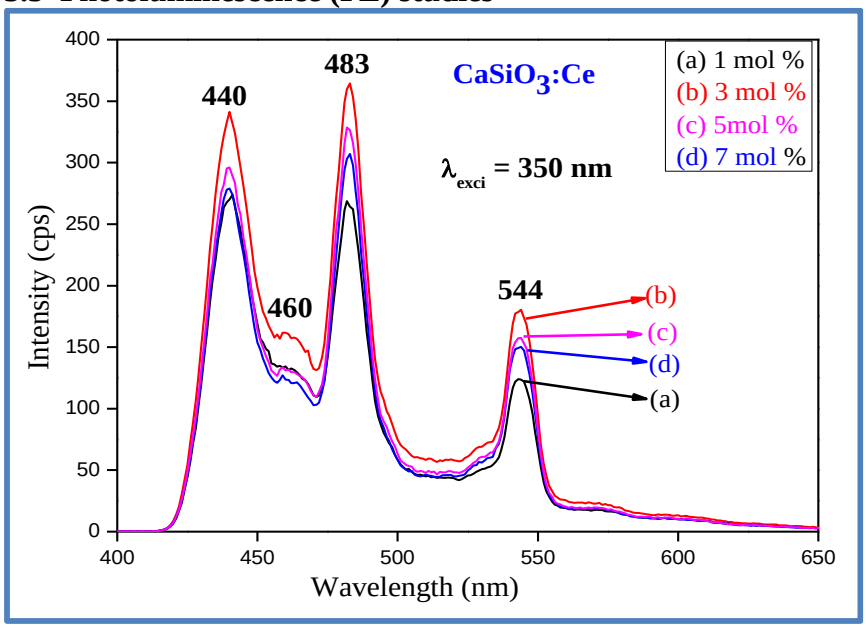

Fig.8. PL Emission spectra of (1-7 mol%) Ce^{3+} substituted $CaSiO_3$ nanophosphor excited at 350 nm.

The emission spectra of (1-7 mol %) $CaSiO_3$:Ce^{3+} nanophosphor measured at 350 nm excitation was shown in the Fig. 8. The emission bands at 440, 460, 483 and 544 nm

observed were attributed to Ce^{3+} ions [23-25]. Strongest emission peak at 483 nm corresponding to 5d → 4f ($2F_{5/2}$) was due to hypersensitive forced electric-dipole transition. The configurationally coordinate model was explaining the shape of the broadband transition. PL intensity variation with different Ce^{3+} concentration was studied and shown in Fig. 9. The figure shows that PL intensity increases with increase in Ce^{3+} concentration up to 3 mol% and thereafter it decrease with further increase in Ce^{3+} concentration and this is understood by concentration quenching due to cross relaxation. As dopant concentration of Ce^{3+} increases, 5d → 4f ($2F_{5/2}$) transition dominates and the emission intensity increases. As Ce^{3+} concentration increases the transition centered at 5d → 4f ($2F_{5/2}$) (483 nm) shows an enhanced emission up to 3 mol % of Ce^{3+}. Similarly, the increase in Ce^{3+} awareness greater than 3 mol % the PL intensity is lower due to concentration quenching. For this reason, the excited atom moves to the quenching sites, dissipating the energy non-radiatively. Due to the concentration quenching the emission intensity decreases. The critical energy transfer distance (R_c) was calculated by,

$$R_c \approx 2\left[\frac{3V}{4\pi X_c N}\right]^{1/3} \text{------(2)}$$

Where X_c; the critical concentration, N; the number of cation sites in the unit cell, and V; the volume of the unit cell. For $CaSiO_3$: Ce^{3+} nanophosphor the values of N, V and X_c were 6, 409.85 $Å^3$ and 0.03 respectively. Using those parameters, the anticipated Rc is observed to be 16.33 Å. considering Rc was not less than 5Å, exchange interaction become not liable for non-radiative energy transfer method from one Ce^{3+} ion to another Ce^{3+} ion on this host.

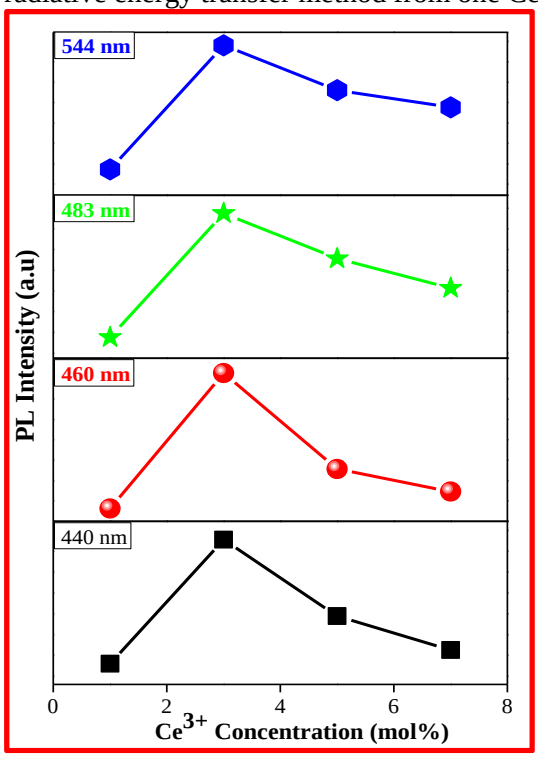

Fig.9. The variation of PL intensity with different Ce^{3+} concentration.

The Blasse theory [26], non-radiative energy among different Ce^{3+} ions in $CaSiO_3$ phosphor might also arise through radiative change multipole-multipole interaction. Typically, the radiative re-absorption mechanism comes into effect while there has been an extensive overlap of emission peaks of the sensitizer and activator. In this example, radiative - reabsorption become completely dominated out as there have been no wide overlapping peaks. Therefore, multipolar interaction changed into used to explain the concentration quenching. Multipolar interaction includes several kinds of interaction consisting of dipole-dipole (d-d), dipole-quadropole (d-q), quadropole-quadropole (q-q) interaction.

As a result, the energy transfer method of Ce^{3+} in $CaSiO_3$ phosphor could be because of multipolar interaction.

In order to decide the type of interaction involved within the energy transfer Van Uitert's [27] proposed an equation:

$$\frac{I}{X} = k\left[1+\beta(X)^{Q/3}\right]^{-1} \text{-----(3)}$$

Where I; the integral intensity of emission spectra from 550-750 nm, X; the activator concentration, I/X; the emission intensity per activator (X), β and K; constants for a given host under same excitation condition. According to above equation, Q = 3 for the energy transfer among the nearest neighbor ions, while Q = 6, 8 and 10 for d-d, d-q and q-q interactions respectively. Assuming that $\beta(X)^{Q/3} >> 1$, above equation can be written as

$$\log\left(\frac{I}{X}\right) = K' - \frac{Q}{3}\log X \,(K' = \log K - \log\beta) \text{-----(4)}$$

From equation (5), the multipolar character (Q) can be obtained by plot log (I/X) vs log (X) as shown in Fig.10. Slope and multipolar character 'Q' was found to be - 0.94 and 2.565 which was close to 6. Therefore, the concentration quenching in $CaSiO_3$: Ce^{3+} phosphor occurred due to dipole to dipole interaction.

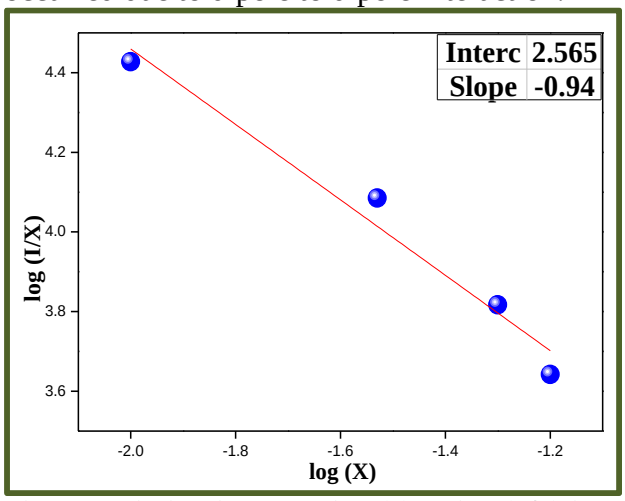

Fig.10. Relation between log (x) vs log (I/x) in $CaSiO_3$:Ce^{3+} nanophosphor.

The Commission International De I-Eclairage (CIE) chromaticity coordinates for $CaSiO_3$: Ce^{3+} (1-7 mol %) nanophosphors as a function of Ce^{3+} concentration for the luminous color was depicted by the PL spectra. The CIE coordinates of blue emission of Ce^{3+} ions not only rely upon the asymmetric ratio but additionally rely on the higher energy emission levels. Literature exhibits that the Ce^{3+} doping effect turns into stronger in the case of particles with higher crystallinity, resulting in an improved activation degree of Ce^{3+}. Their corresponding places were star marked in the blue area in Fig. 11(a), their X and Y values had been given in the table inset of Fig. 11(a).

The Coordinated Color Temperature (CCT) values were well located in the blue region shown in the star mark in Fig. 11(b). The estimated Planckian locus defines the color temperature of a light source and calculated values of CCT shown inset table of Fig. 11(b) by using transforming equations 5 and 6 shows the temperature of the closest point of the Planckian locus to the light source on the (U′, V′) uniform chromaticity diagram (Fig.11(b)).

$$U' = \frac{4x}{-2x+12y+3} \text{----------(5)}$$

$$V' = \frac{9y}{-2x+12y+3} \text{----------(6)}$$

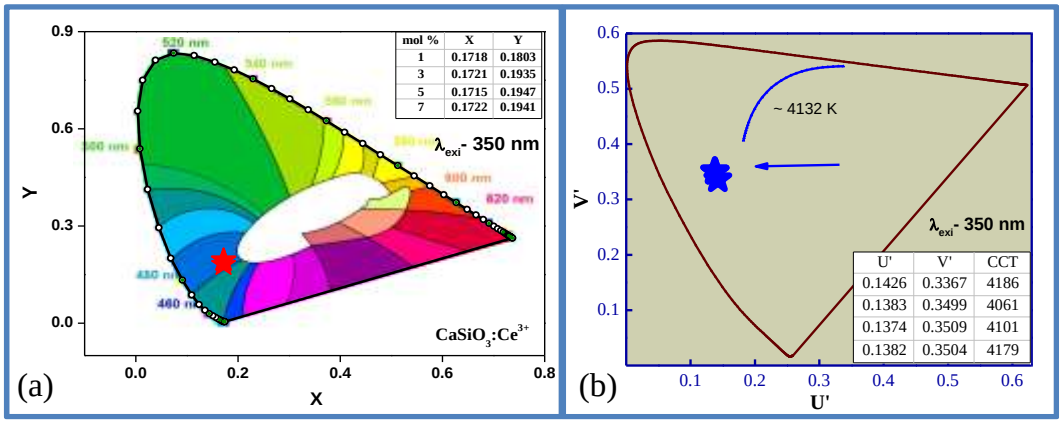

Fig.11 (a). CIE chromaticity diagram of (Inst table: x and y values) (b) CCT (Inst table: u′, v′ and CCT values) of (1-7 mol%) Ce^{3+} substituted $CaSiO_3$ nanophosphor.

The average CCT value of prepared $CaSiO_3:Ce^{3+}$ nanophosphor is 4132 K which was very close to standard NTSC values [28]. This shows that the strongest emission peak indicates at 3 mol % $CaSiO_3$: Ce^{3+} nanophosphor was suitable material for the fabrication of blue element of WLEDs and additionally solid-state display applications.

4. CONCLUSION

$CaSiO_3:Ce^{3+}$ (1-7 mol %) nanophosphor was successfully synthesized via combustion method. The average crystallite size was expected from Scherer's and W-H plots. Emission spectra show that there's an increase in emission intensity with increase in Ce^{3+} attention and beyond 3 mol% concentration quenching is found because of dipole to dipole interaction. Narrow blue emission peak observed at 483 nm in $CaSiO_3:Ce^{3+}$ is due to 5d → 4f ($2F_{5/2}$) transition from Ce^{3+} ions. The CIE chromaticity co-ordinates and CCT situated in the blue region, hence $CaSiO_3:Ce^{3+}$ the phosphor might be useful in blue component of WLEDs and also display applications.

References

[1]. C.B. Palan, K.A.Koparkar, N.S.Bajaj, S.K.Omanwar, **Synthesis and TL/OSL properties of $CaSiO_3$:Ce biomaterial**, Materials Letters, 175 (2016) 288–290

[2]. Bowers MJ, Mcbride JR, Sandra SJ. **White-light emission from magic-sized cadmium selenide nanocrystals,** J. Am. Chem. Soc. 127 (2005) 15378-15379.

[3]. Lei Zhou, Bing Yan, **Sol–gel synthesis and photoluminescence of $CaSiO_3:Eu^{3+}$ nanophosphors using novelsilicatesources**, Journal of Physics and Chemistry of Solids 69 (2008) 2877–2882

[4]. Geng W, Zhou X, Ding J, et al. **NaBaY(BO3)2: Ce^{3+}, Tb^{3+}: a novel sharp green-emitting phosphor used for WLED and FEDs**, J. Am. Chem. Soc. 101 (2018) 4560-4571.

[5]. Huanping Wang, Qilong Zhang, Hui Yang, Huiping Sun, **Synthesis and microwave dielectric properties of $CaSiO_3$ nanopowder by the sol–gel process**, Ceramics International 34 (2008) 1405–1408.

[6]. Sun JY, Zhang XY, Xia ZG, et al. **Synthesis and luminescence properties of novel $LiSrPO_4$: Dy^{3+} phosphor**, Mater. Res. Bull. 46 (2011) 2179-2182.

[7]. Li PL, Wang ZJ, Yang ZP, et al. **Luminescent characteristics of $LiCaBO_3$: M (M = Eu^{3+}, Sm, Tb^{3+}, Ce^{3+}, Dy^{3+}) phosphor for white LED**, J. Lumin. 2010; 130: 222-225.

[8]. Wang JY, Wang JB, Duan P. **Luminescence and energy transfer of Tm^{3+} or/ and Dy^{3+} co doped in $Sr_3Y(PO_4)_3$ phosphors with UV excitation for WLEDs**, J. Lumin. 145 (2013) 1-5.

[9]. Li K, Shang M, Zhang Y, et al. **Photoluminescence properties of single-component white-emitting Ca9Bi(PO4)7: Ce^{3+}, Tb^{3+}, Mn^{2+} phosphors for UV LEDs**, J. Mater. Chem. C. 3 (2015) 7096-7104.

[10]. Yu Teng a, Jiajia Zhou a, Said Nasir Khisro a, Shifeng Zhou a, Jianrong Qiu, **Persistent luminescence of $SrAl_2O_4$: Eu^{2+}, Dy^{3+}, Cr^{3+} phosphors in the tissue transparency window,** Materials Chemistry and Physics, 147 (2014) 772-776.

[11]. K. Suresh, Nannapaneni V. Poorna Chandra Rao and K.V.R.Murthy, **Synthesis and photoluminescence of $Ca_3Si_3O_8F_2$:Ce^{4+}, Eu^{3+}, Tb^{3+} phosphor**, Advances in Materials Research, 3-4 (2014) 227-232.

[12]. I.I. Kindrat, B.V. Padlyak, S. Mahlik, B. Kuklinski, Y.O. Kulyk, **Spectroscopic properties of the Ce-doped borate glasses**, Optical Materials, 59 (2016) 20-27

[13]. Y. Hou, J. Zhang, Z. Ding, L. Wu, Powder Technol., 203 (2010) 440–446.

[14]. K.C. Patil, M.S. Hegde, Tanu Rattan, S.T. Aruna, **Chemistry of Nanocrystalline Oxide Materials, Combustion Synthesis, Properties and Applications**, World Scientific Publishing Co. Pvt. Ltd., Singapore, 2008.

[15]. Lei Zhou, Bing Yan, **Sol–gel synthesis and photoluminescence of $CaSiO_3$:Eu^{3+} nanophosphors using novel silicate sources**, Journal of Physics and Chemistry of Solids, 69-11 (2008) 2877-2882.

[16]. M. Madesh Kumar, H. Nagabhushana, B.M. Nagabhushana, N. Suriyamurthy, S.C. Sharma, C. Shivakumara, R. Hari Krishna, **Synthesis, characterization and spectroscopic investigation of Cr^{3+} doped wollastonite nanophosphors**, Spectrochimica Acta Part A: Molecular and Biomolecular Spectroscopy 128 (2014) 403–407.

[17]. Y.L. Liu, J.Y. Kuang, B.F. Lei, C.S. Shi, J. Mater. Chem., 15 (2005) 4025-4031.

[18]. G.K. Williamson, W.H. Hall, Acta Metall., 1 (1953) 22-31.

[19]. P. Klug, L.E. Alexander, **In: X-ray Diffraction Procedure,** Wiley, New York, 1954.

[20]. B.M. Manohara, H. Nagabhushana, K. Thyagarajan, B. Daruka Prasad, S.C. Prashantha, B. M. Nagabhushana and S.C. Sharma, **Synthesis and Photoluminescence properties of $CdSiO_3$: Ho^{3+} nanophosphor**, Advanced Science Letters, American Scientific Publisher, 22-4 (2016) 785-789.

[21]. A. Escobedo Morales, E. Sanchez Mora, U. Pal, **Use of diffuse reflectance spectroscopy for optical characterization of un-supported nanostructures**, Rev. Mexic. De Fisica S, 53 (2007) 18-22.

[22]. M. Wanga, X. Zhang, Z. Hao, X. Ren, Y. Luo, X. Wang, J. Zhang, **Enhanced Phosphorescence in N Contained Ba_2SiO_4:Eu^{2+} for X-ray and Cathode Ray Tubes**, Opt. Mater., 32 (2010) 1042–1045.

[23]. Dhanu R., D. Prakashbabu, Bindua, M. Madesh Kumar, S. Ponkumar, R. Hari Krishna, K. Mani Rahulan, **Photoluminescence of mixed phase $CaSiO_3$:Ce^{3+} nanophosphors,** Optik - International Journal for Light and Electron Optics, 218 (2020) 165139.

[24]. G.Q. Xu, Z.X. Zheng, W.M. Tang, Y.C. Wu, **Spectroscopic properties of Ce^{3+} doped silica annealed at different temperatures**, J. Lumin., 124 (2007) 151–156

[25]. Meng Lu, Chaofeng Zhu, Zhongtao Chen, Meiling Shi, Xiangeng Meng **Ce^{3+} and Dy^{3+} doped $Ca_3(P_{1-x}B_xO_4)_2$ phosphors for white light-emitting applications,** J. Alloys Compd., 775 (2019) 1044-1051

[26]. G. Blasse, Philips Res. Rep., 24 (1969) 131-144.

[27]. L.G Van Uitert. J. Electrochem. Soc., 114 (1967) 1048-1053.

[28]. B. M. Manohara, H. Nagabhushana, K. Thyagarajan, B. D. Prasad, S.C. Prashantha, S. C. Sharma and B. M. Nagabhushana, **Spectroscopic and luminescence studiesof Cr^{3+} doped cadmium silicate nano-phosphor,** J. Lumin., 161 (2015) 247–256.